



# A new auroral phenomenon: The anti-black aurora

A.E. Nel · M. Kosch

[anel@sansa.org.za](mailto:anel@sansa.org.za)

April 24, 2020

# Discrete and diffuse auroras are well-known bright auroras



Discrete aurora. (Credit: *Nature* 467,927–928, 21 October 2010)

- ▶ Bright, sharply defined curtain-like structure.
- ▶ Pre-magnetic midnight on the nightside auroral oval.

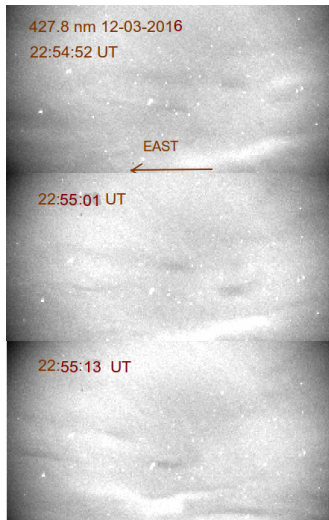


Diffuse aurora. (Credit: *Bob King, Universe Today*, 26 April 2016)

- ▶ Broad band of uniform auroral glow.
- ▶ Relatively constant energy spectrum.
- ▶ Seen post-magnetic midnight moving equatorward.

# Embedded in the diffuse aurora is the black aurora

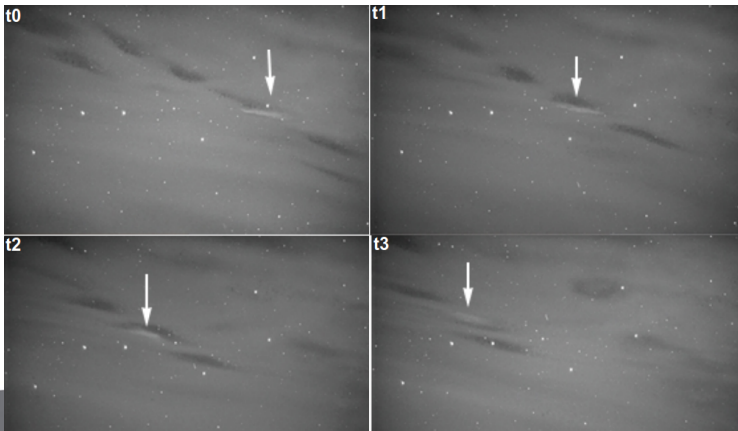
- ▶ At first thought to be dark holes against a diffuse background.
- ▶ Now known to be well-defined, discrete structures <sup>1</sup>, with a lower luminosity than the surrounding diffuse aurora.
- ▶ Various morphologies exist: patches, arc segments and arcs are most prevalent.
- ▶ Example of black aurora patches drifting Eastward during 2016 campaign, Ramfjordmoen Norway.



<sup>1</sup>Trondsen, T., and Cogger, L. L. High-resolution television observations of black aurora. *J. Geophys. Res.* 102, 363-378, 1997

# Anti-black aurora

- ▶ White patch sometimes seen travelling alongside a black aurora.
- ▶ First recorded by Torsten Aslaksen with white light camera outside Trømsø, Norway 2007.
- ▶ Coined by authors as 'anti-black aurora'
- ▶ No studies exist in literature pertaining to this phenomenon.



# Underlying mechanisms and proposed observation methods

- ▶ Several underlying mechanisms have been proposed for black auroras: the coupled ionospheric-magnetospheric generation mechanism<sup>2</sup> and the magnetospheric generation mechanism<sup>3</sup>.
- ▶ The underlying mechanism (as well as energy characteristics, luminosity, and morphology) of anti-black auroras are as of yet unknown.
- ▶ To gather data for analysis of these auroral events, an incoherent scatter radar and dual-wavelength cameras records in parallel over the course of 2 weeks in March 2016 outside Trømsø, Norway.

---

<sup>2</sup>Marklund, G., Karlsson, T., and Clemmons, J. On low-altitude particle acceleration and intense electric fields and their relationship to black aurora. *J. Geophys. Res.* 17, 509 – 17, 522, 1997

<sup>3</sup>Peticolas, L. M., Hallinan, T. J., Stenbaek-Nielsen, H. C., Bonnell, J. W., and Carlson, C. W. A study of black aurora from aircraft-based optical observations and plasma measurements on fast. *J. Geophys. Res.* 107, 2002

# EISCAT facility, Ramfjordmoen Norway



**Figure:** The EISCAT facility outside Trømsø. In the front is the UHF radar used in this study, which operates in the 931 MHz band.

## EISCAT facility, Ramfjordmoen Norway



**Figure:** Running in parallel a few 100 metres from the radar control room are an iXon-888 EMCCD camera mounted with a 427.8 nm filter, and pointing into the magnetic zenith ( $az=180^\circ$ ,  $el=77^\circ$ ) with a  $30^\circ$  field of view (FOV). An ALTA-U47 back-illuminated CCD camera was mounted with a 844.6 nm filter, and pointed into the local zenith with a  $50^\circ$  FOV

Event	Date	UT	Width	Length	Drift velocity
1A	20061022	20:50:22 - 20:51:47	1.00±0.1 km	–	–
1B	20061022	20:51:57 - 20:53:07	0.70±0.1 km	–	–
1C	20061022	20:54:03 - 20:54:13	1.80±0.1 km	–	–
2A	20090125	22:58:12 - 23:01:28	1.47±0.4 km	–	–
2B	20090125	23:42:59 - 23:43:38	3.15±0.4 km	–	–
3A	20160307	23:48:11 - 23:52:50	1.89±0.4 km	–	–
4A	20160310	22:44:17 - 22:46:59	2.10±0.4 km	–	–
4C	20160311	00:07:05 - 00:07:47	3.99±0.4 km	–	–
4D	20160311	00:11:17 - 00:17:24	2.31±0.4 km	7.35±0.4 km	0.32 km.s <sup>-1</sup> E 0.25 km.s <sup>-1</sup> N
4E	20160311	00:16:53 - 00:17:41	1.05±0.4 km (w) 1±0.4 km (b)	13.86±0.4 km	0.22 km.s <sup>-1</sup> E 0.11 km.s <sup>-1</sup> N
5A	20160312	21:45:28 - 21:47:37	11.13±0.4 km	–	–
5B	20160312	21:54:22 - 22:11:13	2.73±0.4 km (w) 2.52±0.4 km (b)	16.40±0.4 km	0.87 km.s <sup>-1</sup> E
5C	20160312	22:11:14 - 22:13:58	4.62±0.4 km	–	–
5D	20160312	22:32:07 - 22:32:37	5.46±0.4 km (w) 3.57±0.4 km (b)	4.00±0.4 km	2.00 km.s <sup>-1</sup> E
5E	20160312	22:51:34 - 22:55:37	2.17±0.4 km	16.19±0.4 km	0.65 km.s <sup>-1</sup> E
5F	20160312	22:55:46 - 23:00:22	1.79±0.4 km	14.49±0.4 km	0.95 km.s <sup>-1</sup> E
5G	20160312	23:00:23 - 23:04:04	0.82±0.4 km	–	–
5H	20160312	23:05:43 - 23:06:19	0.93±0.4 km (w) 0.92±0.4 km (b)	17.70±0.4 km	2.26 km.s <sup>-1</sup> E
5I	20160312	23:06:20 - 23:15:52	1.18±0.4 km (w) 1.22 km±0.4 (b)	–	–
5J-1	20160312	23:15:53 - 23:26:01	4.71±0.4 km	–	–
5J-2	20160312	23:15:53 - 23:26:01	1.24±0.4 km (w) 1.49 km±0.4 (b)	13.53±0.4 km	–

**Figure:** Events recorded during 2016 campaign by authors, as well as black aurora events recorded by Archer<sup>4</sup>, and Björn Gustavsson (UiT The Arctic University of Norway), which will be analysed and make part of results.

---

<sup>4</sup>Archer, J., H. Dahlgren, N. Ivchenko, B. S. Lanchester, and G. T. Marklund, Dynamics and characteristics of black aurora as observed by high-resolution ground-based imagers and radar, *International Journal of Remote Sensing*, 32(11), 2973–2985, 2011

# Method to determine characteristic energy of auroral events

- ▶ Infer  $E_c$  from both the radar<sup>5</sup> and optical<sup>6</sup> measurement and compare (2.5 keV).

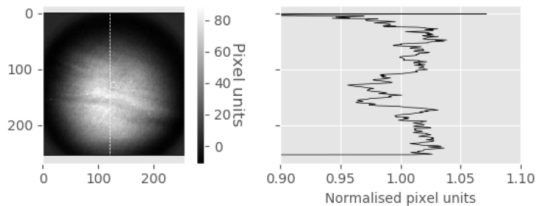


**Figure:** Sample frame from 427.8 nm camera on 2016-03-07. The dotted circle represents the EISCAT beam projected to 105 km, and each frame has a field of view of  $30^\circ \times 30^\circ$ . The frame on the left-hand side are given in pixel coordinates. The dotted line represents the intensity sampling line shown in the right-hand graph.

---

<sup>5</sup>Virtanen, I. I., B. Gustavsson, A. Aikio, A. Kero, K. Asamura, and Y. Ogawa, Electron energy spectrum and auroral power estimation from incoherent scatter radar measurements, *JGR*, 123, 2018

<sup>6</sup>Rees, M. H., and D. Luckey, Auroral electron energy derived from ratio of spectroscopic emissions., *JGR*, 79(34), 5181–5186, 1974

# Anti-black aurora

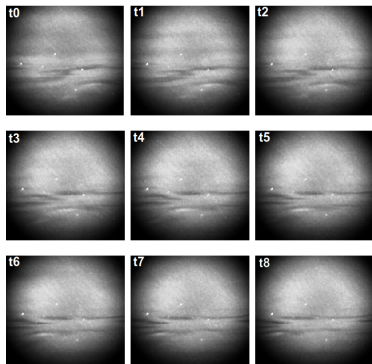
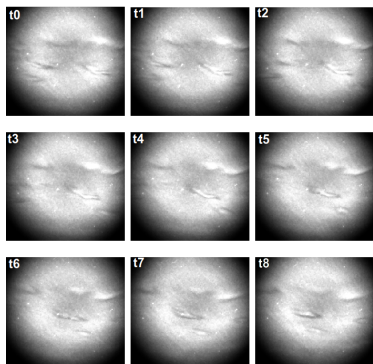


**Figure:** Sample frames of anti-black auroras recorded during 2016 campaign.

# Anti-black aurora

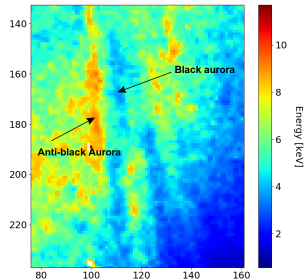
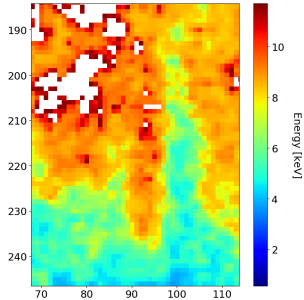


Figure: Characteristic energy maps for anti-black aurora events shown in previous slide.

## Results

- ▶ The anti-black auroras morphology is very similar to that of the black auroras.
- ▶ For an assumed altitude of 105 km, the average horizontal width and length of the anti-black aurora was 2.1 (1.5) and 13.3 (4.4) km, respectively, where the values in brackets refer to the standard deviation.
- ▶ The mean drift speed of the anti-black aurora was 1.3 (0.8) km/s eastward.
- ▶ The optical intensity of the anti-black aurora was on average 10% and 6% brighter than the surrounding diffuse aurora in 427.8 and 844.6 nm, respectively.
- ▶ The optical intensity of the black auroras was on average 24% and 16% less than the surrounding diffuse aurora for 427.8 and 844.6 nm, respectively.
- ▶ For the anti-black aurora events from 12 March 2016, the average mean energy of the black, anti-black and diffuse background auroras was 4.8 (0.8), 11.0 (2.5), and 7.2 (1.1) keV, respectively.

# Conclusion

- ▶ There is never any evidence that the anti-black aurora drifts faster than the black aurora despite its higher mean electron energy.
- ▶ This does not correspond to the gradient-curvature drift of the source plasma in the equatorial magnetosphere (i.e.  $\propto$  energy  $\implies \propto$  drift speed)
- ▶ Mechanism for the anti-black aurora is likely a more local modification of the electron energy at lower altitudes (electrostatic potential drop along B-field lines).

# Summary

- ▶ Previous studies have pointed towards a magnetospheric mechanism responsible for drifting black aurora events where, due to gradient-curvature drift, the velocity of the event as observed in the ionosphere is dependent on the energy of the precipitating particles, i.e., the higher the energy of the precipitating particles, the faster the black aurora patches drift.
- ▶ It is possible that source particles energy within the black aurora is consistent with the motion of the gradient-curvature drift of the source plasma in the magnetosphere, but that each black and anti-black aurora pair contains an upward and downward, respectively, field-aligned current. This needs to be investigated.

## Future work

- ▶ In situ satellite data is needed.
- ▶ Most satellites in this study were found to be in geostationary orbit, with L-shell 6.2, but field lines stretch out to  $10 R_E$  during geomagnetic storms
- ▶ Several satellites do have particle sensors on board that are able to detect cold plasma populations, but only Geotail has an orbit that crosses the region where the possible host electron population are.
- ▶ Observing local electron density enhancements and depletions, that corresponds with upward and downward FAC's
- ▶ EISCAT's radar plasma density observations and ground-based optical observations can be made whilst simultaneous in-situ Geotail satellite data is recorded in the magnetosphere
- ▶ EISCAT 3D project underway

Geotail time range (UT)	$X_{GSE}$ range ( $R_E$ )	$Y_{GSE}$ range ( $R_E$ )	$Z_{GSE}$ range ( $R_E$ )
2019-02-06 17:00 - 19:00	-12 to -10	2 to -2	-1 to 1
2019-02-11/12 23:00 - 01:00	-11 to -10	2 to -1	-1 to 1
2019-02-17 04:00 - 05:30	-11 to -10	2 to 0	0 to 0.5
2019-02-22 10:00 - 13:00	-8 to 10	2 to -3	0 to 2
2019-02-27 15:00 - 18:00	-10 to -9	3 to -2	0 to 2